XMM-Newton CCF Release Note

XMM-CCF-REL-271

EPIC-pn Long-Term CTI

M.J.S. Smith, M. Guainazzi, M. Cappi

December 21, 2010

1 CCF Components

Name of CCF	VALDATE	EVALDATE	Blocks Changed	CAL Version	XSCS Flag
EPN_CTI_0023.CCF	2000-01-01T00:00:00		LONG_TERM_CTI		NO

2 Changes

The T_COEFF vector column in the LONG_TERM_CTI extension contains the parameters to correct the long-term charge transfer inefficiency (CTI) effects. There are individual vectors per mode and CCD, with each vector containing the coefficients of a cubic polynomial in time.

The long-term CTI is implemented as an incremental, time-dependent energy correction, on top of the standard CTI-model energy reconstruction. As new in-flight calibration observations are performed, the long-term CTI parameters are adjusted better to fit the data. In this CCF release, the parameters are additionally modified in order to work with an improved long-term CTI correction algorithm which has been implemented in SAS version 10.

2.1 New long-Term CTI Correction Algorithm

The long-term CTI correction algorithm has been changed in SAS version 10. In earlier SAS versions, the long-term CTI correction was based on an approximative method with a linear dependency on the event RAWY coordinate. The new implementation has an exponential dependence on RAWY and as such is a more exact CTI correction. Moreover, there is now a direct relationship between the coefficients of the polynomial fit to the CTI trend, and the parameters contained in the CCF.

Old algorithm:

$$E_{Corr} = E \left[1 + (a + bt + ct^2 + dt^3)\ \texttt{RAWY}\right]$$

New algorithm:

$$E_{Corr} = E \left[\frac{1-a}{1-(a+bt+ct^2+dt^3)}\right]^{\texttt{RAWY}}$$

Where:

E	is the event energy before long-term correction
E_{Corr}	is the event energy after long-term correction
t	is time
RAWY	is the event RAWY coordinate
a, b, c and d	are the parameters in the T_COEFF vector of the CCF

The new algorithm has not required a change in the CCF structure with respect to the previous CCF issue (0022). However, the parameter values are obviously only meaningful in combination with their respective algorithms; this pairing of CCF parameters with SAS algorithm is controlled through the ALGOID attribute of the LONG_TERM_CTI extension (the ALGOIDs for the old and new algorithm are "2" and "3" respectively). Although SAS version 10 is backwards compatible with the previous issue EPN_CTI_0022.CCF, this new CCF issue requires as a minimum SAS version 10.

2.2 Long-Term CTI Trend

At a given energy, the in-orbit temporal behaviour of the pn CTI can be well parametrised by a 2$^{\text{nd}}$ order polynomial. These best fit polynomial coefficients could ideally be directly used as the long-term CTI parameters in the CCF. However, investigations show that the energy reconstruction using the new algorithm combined with the parameters derived from the modelled long-term CTI trend still show a temporal dependence, which expresses itself as an increasing energy over-correction. It has been verified that this time dependence cannot be due to the long-term CTI correction. The origin of the incorrect energy reconstruction is unknown, and is under investigation.

2.3 Empirical Long-Term CTI Correction

Until this issue is resolved, the following interim solution is implemented in order to obtain adequate energy reconstructions. Instead of deriving the long-term CTI correction parameters from the measured CTI trend, we derive the parameters phenomenologically through a modelling of the *non*-long-term CTI corrected line centroid trends. In fact, this method is similar in principle to how the parameters were determined in previous CCF issues.

The method is illustrated in Fig. 1. The data show the Mn-K$_\alpha$ line centroids as determined

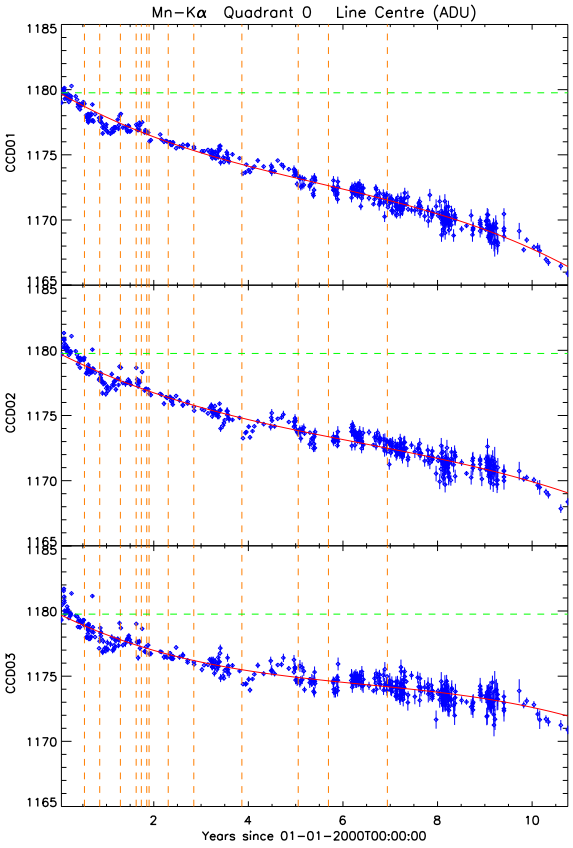

Figure 1: Mn-K_α line centroid energies (in ADU) as determined from Full Frame Mode CalClosed observations, without applying any long-term CTI correction. Only data for Quadrant 0 shown, Quadrants 1, 2 and 3 show similar trends. The horizontal green dashed line shows the theoretical line energy, the vertical dashed lines indicate the times of major solar coronal mass ejections. The overlaid red line is the best fit phenomenological model, which is used to determine the parameter values of the empirical long-term CTI correction. The data shown here were extracted from the complete CCD.

without any long-term CTI correction. To determine the empirical long-term CTI parameters, these data are modelled with the function:

$$f(t) = E_{th}\left[\frac{1-(a+bt+ct^2+dt^3)}{1-a}\right]^{\overline{\texttt{RAWY}}}$$

Where:

E_{th}	is the theoretical line centroid energy
t	is time
$\overline{\texttt{RAWY}}$	is the weighted mean event RAWY coordinate in the area from which the data are extracted
a, b, c and d	are the free parameters

In general, an acceptable model requires a non-zero cubic term (parameter d).

The best fit parameters of this empirical correction will depend on the area of the CCD from

which the data were extracted. As the on-board calibration source illuminates large parts of the detector, one may determine the best fit model in various areas of the CCDs, thus optimising the energy reconstruction for the selected areas to the detriment of that of the remaining parts of the detector. In order to optimise the energy reconstruction for targeted sources, the area chosen for CCD 4 is that restricted to around the boresight (RAWY in the range [181..200]). For the other CCDs, the complete CCD area is used. The resulting model parameters are those which have been used in the new CCF for Full Frame Mode.

Although in the case of Extended Full Frame Mode there are fewer CalClosed observations, there is still sufficient data to perform a similar analysis, and the relevant CCF parameters for this mode are derived from best-fit models to this data.

For Large Window, Small Window, Timing and Burst Mode data there is insufficient CalClosed data to determine model parameters over an acceptable baseline. Moreover, these modes are not designed for full-frame illumination thus complicating the interpretation of CalClosed data. As an approximation, for these modes we use the Full Frame Mode parameters.

3 Scientific Impact and Estimated Quality

3.1 Analysis of CalClosed Data

It follows from the above that using a CCF based on the empirical long-term CTI correction, the energy reconstruction accuracy will depend on the region from which the data are extracted. In particular, the new CCF values are optimised for data extracted from the boresight area. The following plots show the reconstructed Mn-K_α line centroid energies for data extracted from the complete CCD area, and also for data extracted from around the boresight. The results of the new CCF are compared with those of the previous issue.

The Full Frame Mode results using the old CCF are shown in Fig. 2 (data extracted from the complete CCDs) and Fig. 4 (left panel, data extracted from around the boresight). The respective Full Frame Mode results using the new CCF are shown in Fig. 3 and Fig. 4 (right panel).

Using the new CCF, for CCDs in Quadrants 0, 1 and 2 (except CCD 4) the full-CCD extracted data show energy reconstruction stability to within ± 10 eV (equivalent[1] to ± 2 ADU) of the theoretical line energy, except for distinct periods (up to approximately 2001) with slightly higher deviations. Quadrant 3 is not well illuminated by the in-flight calibration source, and hence the energy reconstruction is subject to larger statistical errors. Nevertheless, CCDs 10 and 11 show an energy reconstruction stability to within ± 15 eV. The data extracted for CCD 4 around the boresight show an energy reconstruction stability which in general lies within $+10 / -15$ eV of the theoretical line energy.

The results of the new CCF show a marked improvement with respect to the old CCF, both for the complete CCDs as for the boresight region. For the full CCD data, the improvements are seen

[1] The conversion is: 1 ADU = 5 eV

especially in recent observations. Post revolution $\sim$ 1800 (October 2009), the old CCF results in Mn-K$_\alpha$ line centroid energies dropping systematically below the theoretical value by up to 20 eV in Quadrants 0, 1 and 2. The CCD 4 boresight region results have been improved for all observations: the old CCF results in a systematically low Mn-K$_\alpha$ line centroid energies by 10 eV, with observations since revolution $\sim$ 1600 (September 2008) dropping to 30 eV below the theoretical value.

The Extended Full Frame Mode results for the new CCF are shown in Fig. 5 (data extracted from the complete CCDs) and Fig. 6 (data extracted from around the boresight). The results of the new CCF for Extended Full Frame Mode data are similar to, and in fact slightly better than the Full Frame Mode data with a stability within $\pm$10 eV of the theoretical energy.

3.2 Scientific Validation

Several recent Small Window Mode observations of AGN have been used to validate the new CCF (see Figs. 7 and 8)[2]. The results are qualitatively consistent with those obtained from the Full Frame CalClosed data.

Analysis of Fe-K emission line energies shows that the use of the old CCF results in significantly lower pn energies with respect to those obtained with the EPIC-MOS cameras, by up to 60 eV. Application of the new CCF leads to consistent results between pn and MOS.

4 Expected Updates

The pn CTI will continue to develop in time. Model parameters will likely have to be adjusted to the results of new calibration observations.

An understanding of why the energy correction based purely on the modelling of the long-term CTI trend does not adequately work may lead to new CCF parameters.

5 Test Procedures and Results

Scientific testing and validation described above.

Verification of functionality of EPN_CTI_0023.CCF with SAS 10: `calview`, `cifbuild`, `epproc`. Additionally, functionality test of EPN_CTI_0022.CCF with SAS 10 for backwards compatibility.

[2]The observation numbers and source names are not disclosed because the data are still covered by proprietary rights

6 Acknowledgements

We thank the PIs of the observations referred to in Figs. 7 and 8 for kindly allowing us to use and present some of their results prior to publication.

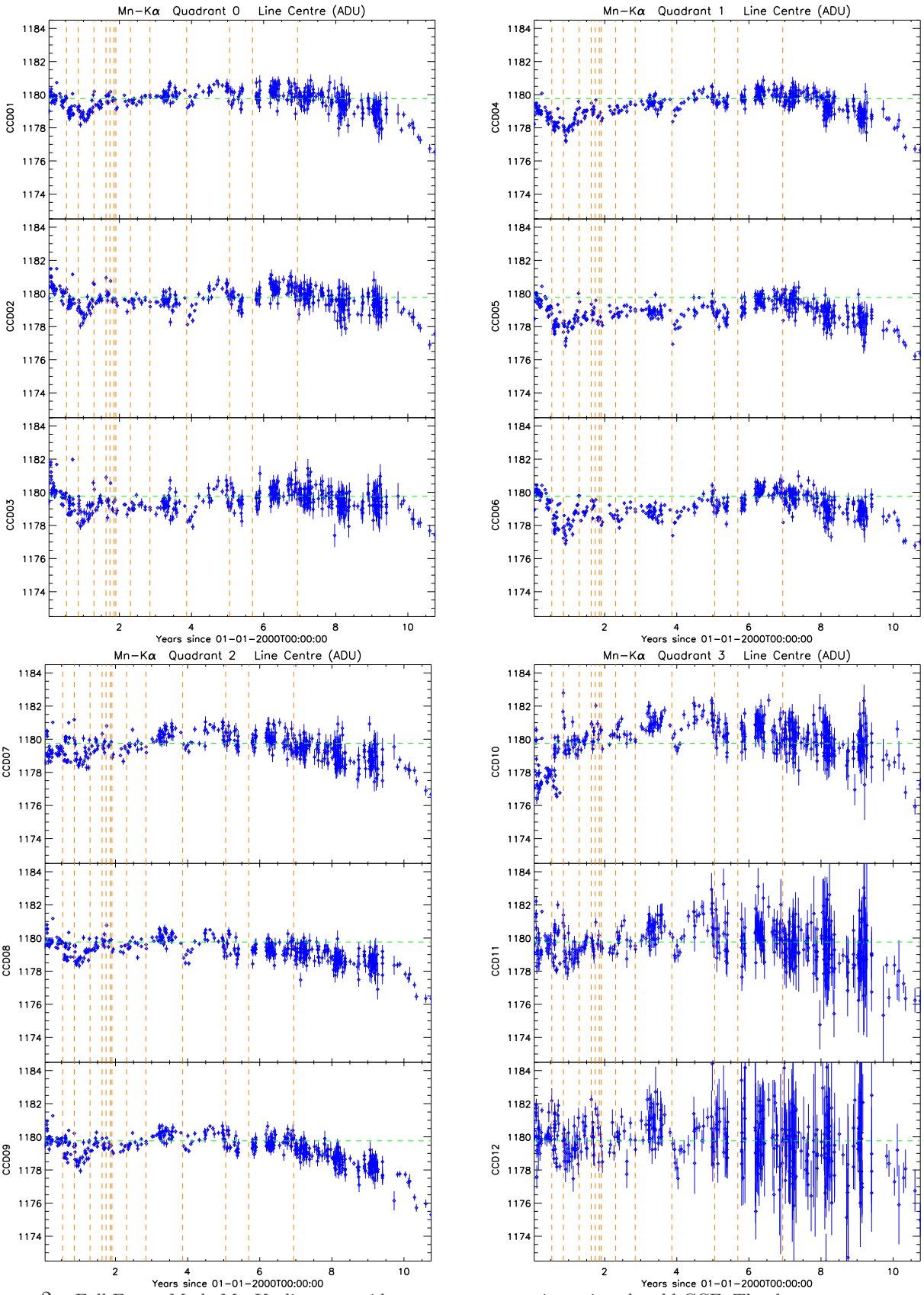

Figure 2: Full Frame Mode Mn-K_α line centroid energy reconstruction using the old CCF. The data were extracted from the well illuminated parts of the complete CCDs. The green dashed line shows the theoretical energy. Post revolution $\sim$ 1800 (October 2009), the old CCF results in Mn-K_α line centroid energies dropping systematically below the theoretical value by up to 20 eV.

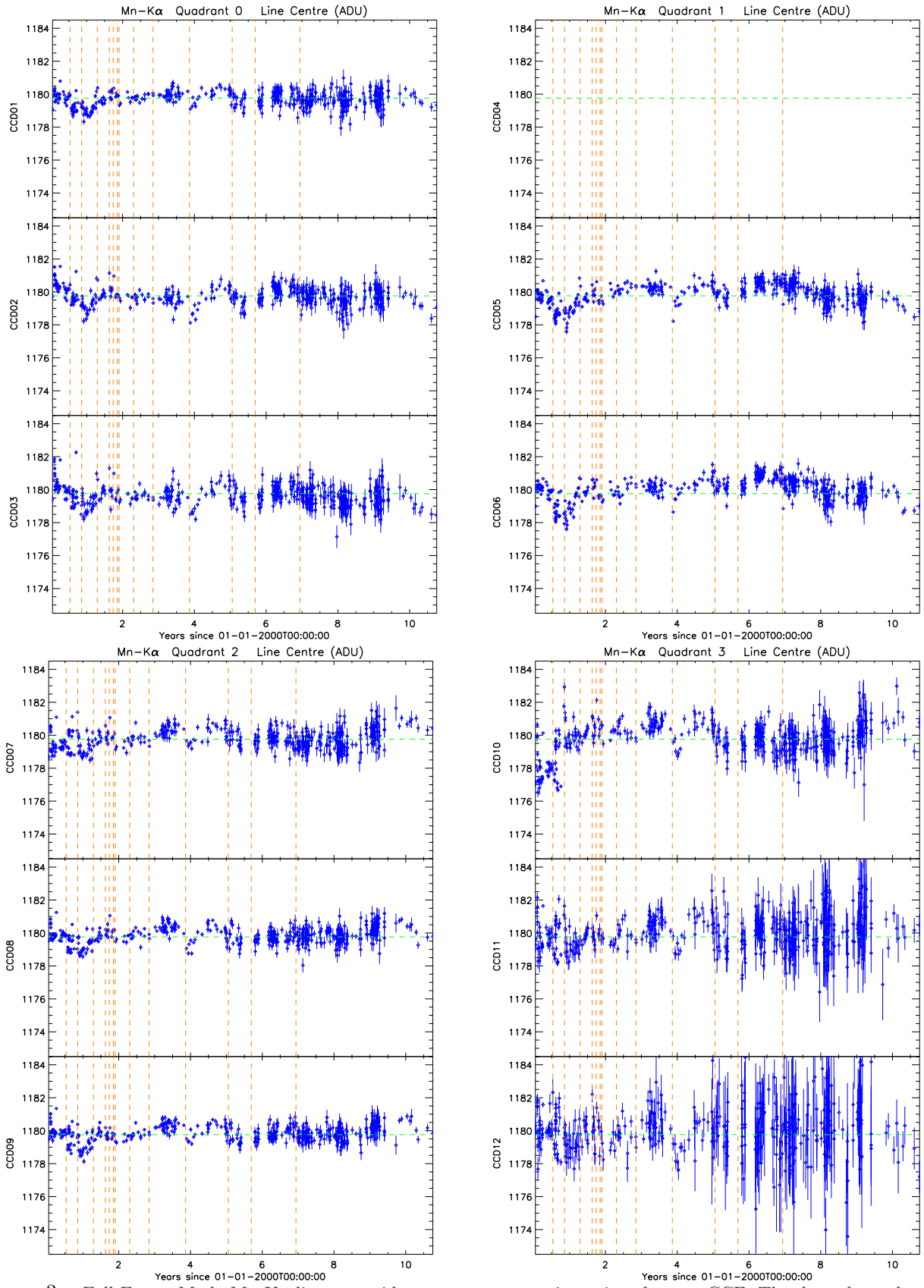

Figure 3: Full Frame Mode Mn-K_α line centroid energy reconstruction using the new CCF. The data shown here were extracted from the well illuminated parts of the full detector. The CCF parameters are optimised for this area for all CCDs except for CCD 4 (which has parameters optimised for data extracted around the boresight and is not shown in this figure). The green dashed line shows the theoretical energy. The reconstructed energy stability is generally within ±15 eV, and for CCDs 1 to 9 (except CCD 4) within ±10 eV, except for distinct periods up to ∼ 2001.

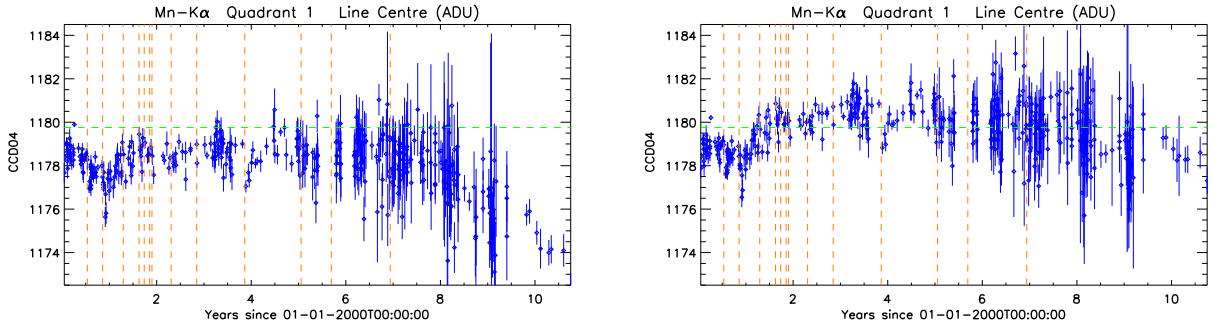

Figure 4: Full Frame Mode Mn-K$_\alpha$ line centroid energy reconstruction with data extracted from the area around the boresight. The green dashed line shows the theoretical energy. Left and right panels show the results obtained with the old and new CCF respectively. The old CCF shows systematic deviations in later observations of up to −30 eV. The new CCF shows a significant improvement, with the reconstructed energy averaging close to the theoretical value, and in general deviating from it by less then ±10 eV.

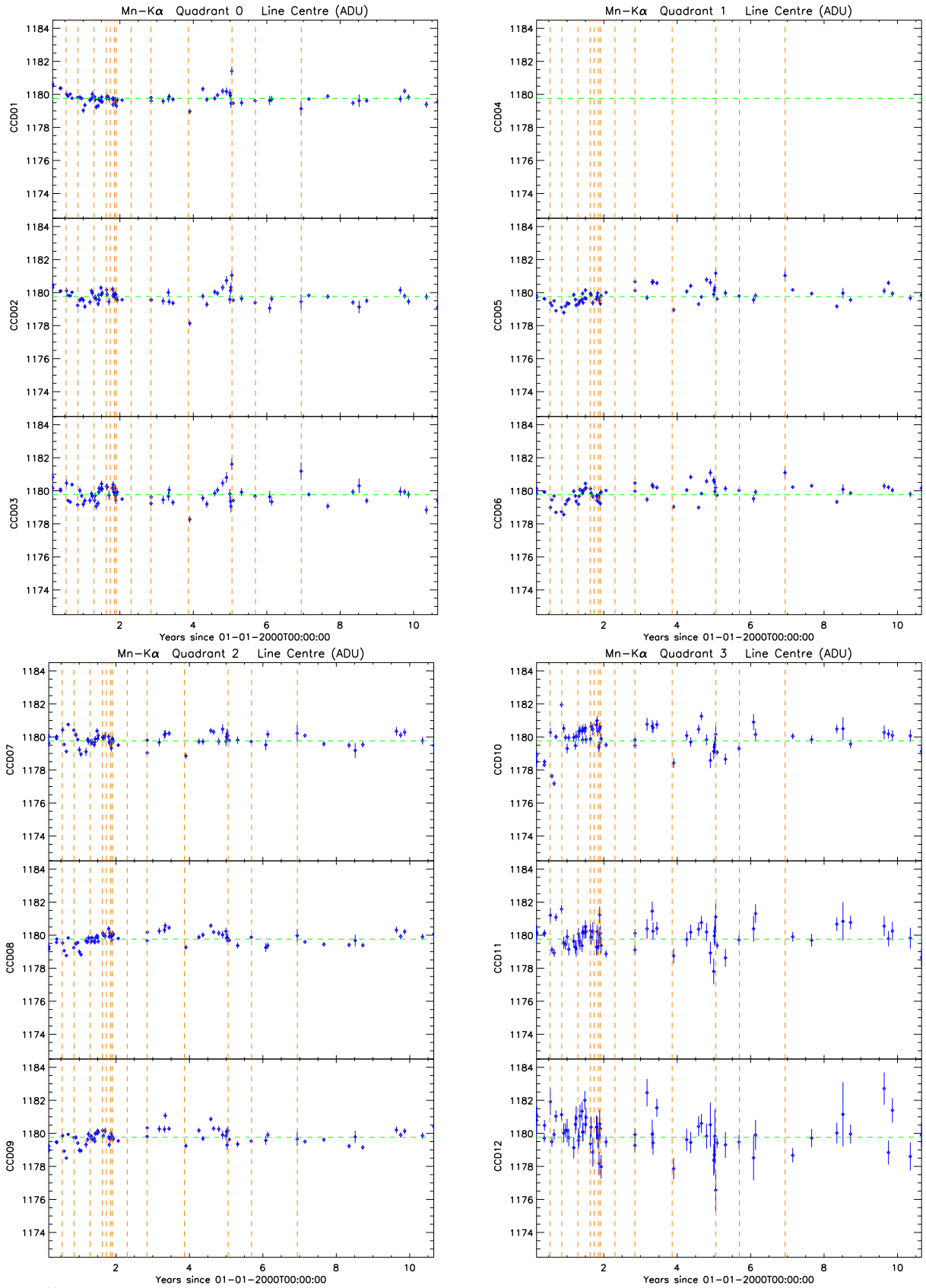

Figure 5: Extended Full Frame Mode Mn-K$_\alpha$ line centroid energy reconstruction using the new CCF. Here, data were extracted from the well illuminated parts of the full detector. The CCF parameters are optimised for this area for all CCDs except for CCD 4 (which is not shown in this figure). The green dashed line shows the theoretical energy. In general, the line stability is within ±10 eV of the theoretical energy.

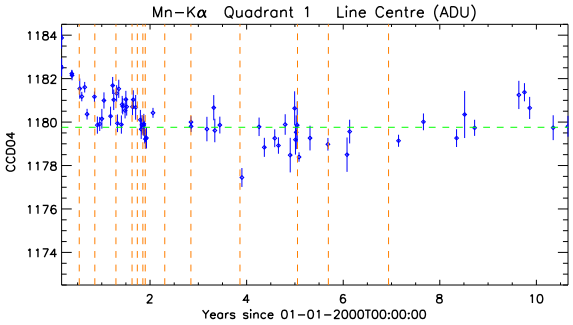

Figure 6: Extended Full Frame Mode Mn-K$_\alpha$ line centroid energy reconstruction using the new CCF, with data extracted from the area around the boresight. The green dashed line shows the theoretical energy. In general, the line stability is within ±10 eV of the theoretical energy.

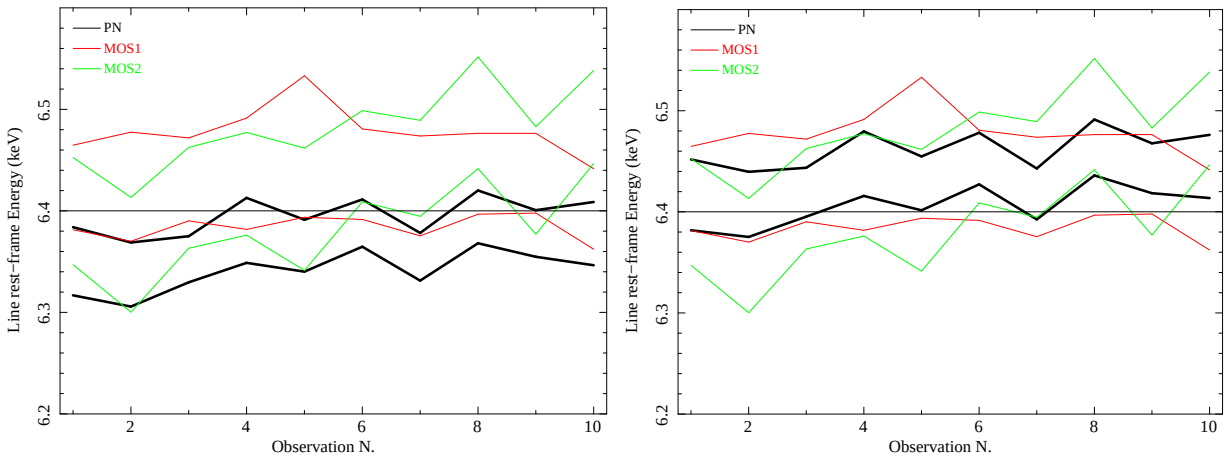

Figure 7: Fe-K line energies, as expressed by the 68% upper and lower confidence limits, determined for 10 Small Window Mode observations of a Seyfert galaxy observed in 2009. The data are of MOS1 (green), MOS2 (red) and pn (black). The left and right panels show results for the old and new CCF, respectively. The old CCF results in a significant systematic pn redshift with respect to the MOS data. The new CCF shows consistent results between pn and MOS. The centroid energy is formally inconsistent with the laboratory energy of the neutral Fe-K$_\alpha$ fluorescence line. This is most likely an astrophysical effect. However, more data from different astrophysical sources are required to reach a conclusion on this point (cf. also Fig. 8).

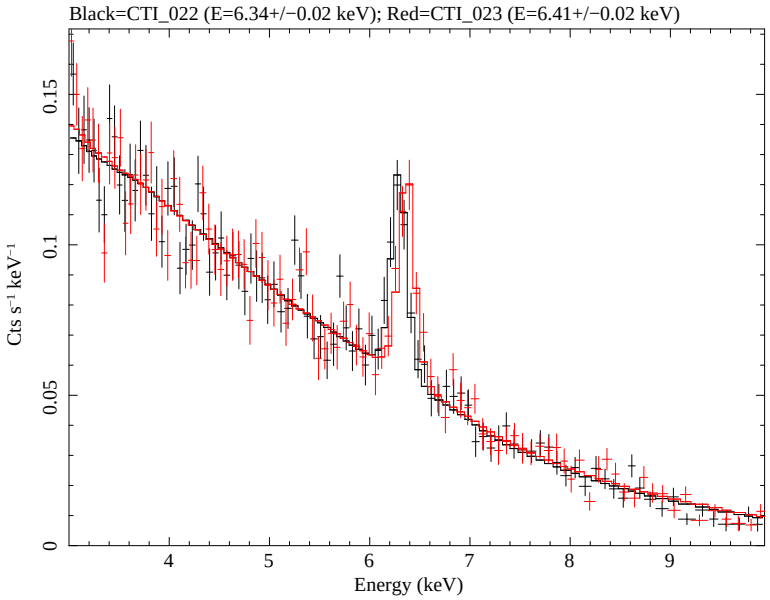

Figure 8: pn Small Window Mode data and best fit model around an emission line of a Seyfert 2 galaxy observed in 2010. The results obtained with the old and new CCFs are shown in black and red respectively. The old CCF results in a line centroid energy which is significantly lower than the laboratory energy of neutral Fe-K$_\alpha$ (6.4 keV), which, on astrophysical grounds, would be the expected energy. Results with the new CCF are consistent with the theoretical energy, and, furthermore, consistent with the line energy as measured by the EPIC-MOS cameras (6.40 $\pm$ 0.02 keV; PI, private communication).